Spin Polarization of Quantum Well States in Ag Films Induced by the Rashba Effect at the Surface

Ke He,[1,2] Toru Hirahara,[2] Taichi Okuda,[1] Shuji Hasegawa,[2] Akito Kakizaki,[1] and Iwao Matsuda[1]

[1]*Institute for Solid State Physics (ISSP), the University of Tokyo, 5-1-5 Kashiwanoha, Chiba 277-8581, Japan*

[2]*Department of Physics, School of Science, the University of Tokyo, 7-3-1 Hongo, Bunkyo-ku, Tokyo 113-0033, Japan*

(Received 8 June 2008; published 5 September 2008)

The electronic structure of Ag(111) quantum well films covered with a $(\sqrt{3} \times \sqrt{3})$ $R30°$ Bi/Ag surface ordered alloy, which shows a Rashba spin-split surface state, is investigated with angle-resolved photoemission spectroscopy. The band dispersion of the spin-split surface state is significantly modified by the interaction with the quantum well states of Ag films. The interaction is well described by the band hybridization model, which concludes the spin polarization of the quantum well states.

DOI: 10.1103/PhysRevLett.101.107604 PACS numbers: 79.60.−i, 73.20.−r

One of the most important issues in spintronics is how to generate and control spin-polarized electrons with electrical methods [1]. The Rashba effect [2], which originates from spin-orbit interaction, can produce a spin-split energy band in a nonmagnetic material and be modified by an electrical voltage and therefore plays a crucial role in various fields of spintronics such as spin relaxation [3], the spin field-effect transistor [4], and the spin Hall effect [5–7]. In recent years, the surface states (SSs) of some heavy metal crystals, for example, Au [8], Bi [9], and Sb [10], were reported to show rather large Rashba splittings compared with bands in conventional semiconductor-based devices [11]. However, since in metals the electrons from SSs account only for a small portion of the whole conduction electrons, except for rare cases [12], the large Rashba spin splitting cannot be expected to significantly influence the overall electronic transport properties of the host metals. In this Letter, we demonstrate that in a metal quantum well film with a Rashba spin-split SS, through the hybridization between quantum well states (QWSs) and the SS, the influence of the Rashba effect can be introduced from the electrons localized at the surface to electrons throughout the whole film. Hybridizations between SSs, QWSs, and substrate bands have been reported in many elemental metal quantum well films [13–17], among which Ag(111) film is one of the best studied [13,14,18]. The SS of the $(\sqrt{3} \times \sqrt{3})$ $R30°$ Bi/Ag ordered surface alloy on Ag (111) has the largest Rashba spin splitting reported so far [19]. In this work, we prepared $(\sqrt{3} \times \sqrt{3})$ $R30°$ Bi/Ag on surfaces of Ag(111) quantum well films. Our angle-resolved photoemission spectroscopy (ARPES) results show clear hybridization behavior between the SS of $(\sqrt{3} \times \sqrt{3})$ $R30°$ Bi/Ag and the QWSs of Ag films. The simulation based on the band hybridization model exhibits the spin polarization of the QWSs as the result of the interaction. The present Letter provides a new method of using the Rashba effect to fabricate spin-polarized band structure in regions other than the surface and interface.

Experiments were performed in an UHV chamber equipped with systems of reflection high-energy electron diffraction and ARPES. ARPES measurements were carried out with an unpolarized He I light source and a Gammadata Scienta SES-100 analyzer at the energy resolution of 35 meV. Ultrathin Ag(111) films [11–22 monolayers (ML) thick; 1 ML: 2.36 Å] are fabricated by depositing Ag at 150 K on Si(111)7 × 7 and postannealing to room temperature [13]. The $(\sqrt{3} \times \sqrt{3})$ $R30°$ Bi/Ag ordered surface alloy is obtained by depositing 1/3 ML Bi onto a Ag(111) film at 400 K.

Figure 1(a) shows the normal-emission photoelectron spectra of a 15 ML Ag(111) film before (bottom) and after (top) Bi deposition. For the spectrum of the clean Ag film, a sharp peak at Fermi level (E_F) is assigned to the SS of Ag

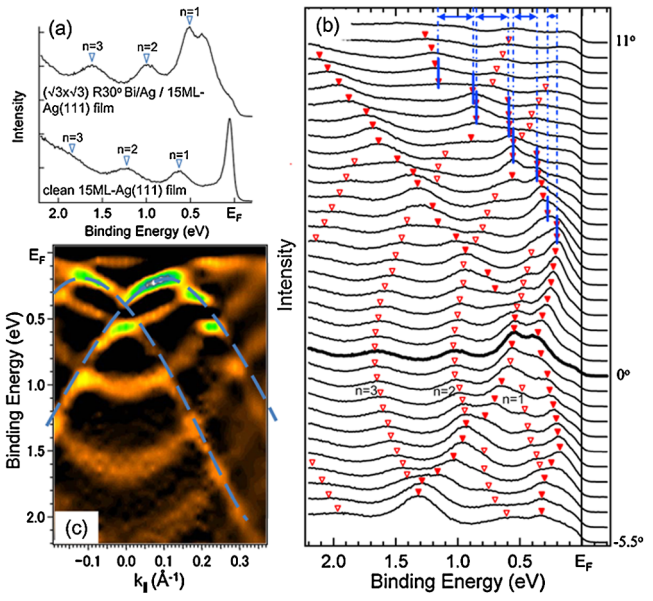

FIG. 1 (color online). (a) Normal-emission photoemission spectra of a 15 ML Ag(111) film with clean (bottom) and $(\sqrt{3} \times \sqrt{3})$ $R30°$ Bi/Ag (top) surfaces. (b) ARPES spectra of the $(\sqrt{3} \times \sqrt{3})$ $R30°$ Bi/Ag covered 15 ML Ag(111) film. (c) Gray-scale $E_B - k_{\|}$ map obtained from (b). The dashed blue lines indicate the band dispersion of the SS bands of $(\sqrt{3} \times \sqrt{3})$ $R30°$ Bi/Ag on Ag(111) bulk crystal.

(111), while peaks at binding energies (E_B) of 0.5–1.5 eV are QWSs [13]. Through the formation of the $(\sqrt{3}\times\sqrt{3})$ $R30°$ Bi/Ag surface, the Ag(111) SS peak is suppressed and a new peak emerges at $E_B \sim 0.36$ eV, which is equal to the SS peak of $(\sqrt{3}\times\sqrt{3})$ $R30°$ Bi/Ag at the $\bar{\Gamma}$ point [19]. The three peaks with higher binding energies indicated by hollow triangles are QWSs, since they will shift towards the Fermi edge with increasing film thickness as will be shown below. The energy positions of the QWSs in the Ag (111) film with $(\sqrt{3}\times\sqrt{3})$ $R30°$ Bi/Ag surface are different from those in the clean Ag(111) film. The energy shifts of the QWSs are likely due to a change of the reflection phase shift of an electron at the film-vacuum interface in the quantization condition [18] induced by $(\sqrt{3}\times\sqrt{3})$ $R30°$ Bi/Ag structure.

Figure 1(b) shows a set of ARPES spectra measured along the $\bar{\Gamma}\bar{M}$ direction of the surface Brillouin zone of a 15 ML Ag(111) film covered with $(\sqrt{3}\times\sqrt{3})$ $R30°$ Bi/Ag. The experimental $E_B - k_{\|}$ diagram of in-plane dispersion, fabricated by the second derivatives of the spectra in Fig. 1(b), is shown in Fig. 1(c). One can observe many bands sharply dispersing through the measured energy range. The parabolic bands, which disperse towards the Fermi level with wave vectors [indicated with hollow triangles in Fig. 1(b)] correspond to QWS subbands. As for the bands dispersing to higher binding energies with wave vectors [indicated with solid triangles in Fig. 1(b)], the energy positions are roughly consistent with the spin-split SS of $(\sqrt{3}\times\sqrt{3})$ $R30°$ Bi/Ag on Ag(111) bulk, as depicted in Fig. 1(c) with dashed blue lines, except around crossings with the QWS bands where the dispersions become flat and energy splittings can be observed. The energy splittings in the bands near the $\bar{\Gamma}$ point are less obvious than those with larger wave vectors. The band dispersions along the $\bar{\Gamma}\bar{K}$ direction are essentially similar to that of the $\bar{\Gamma}\bar{M}$ direction (not shown here).

Figure 2 shows a series of $E_B - k_{\|}$ diagrams of $(\sqrt{3}\times\sqrt{3})$ $R30°$ Bi/Ag covered Ag(111) films at different thicknesses. The QWS subbands move towards the Fermi level with increasing film thickness as found in other QWS systems [18]. The positions of the energy splittings move correspondingly with the QWSs. The sizes of the splittings decrease with increasing film thickness for the same QWS band. At the very thick film that has no QWS, we can observe only the SS band of $(\sqrt{3}\times\sqrt{3})$ $R30°$ Bi/Ag just as in the bulk case [19]. The above observations demonstrate that the energy splittings are results of the interaction between QWSs and spin-split SSs.

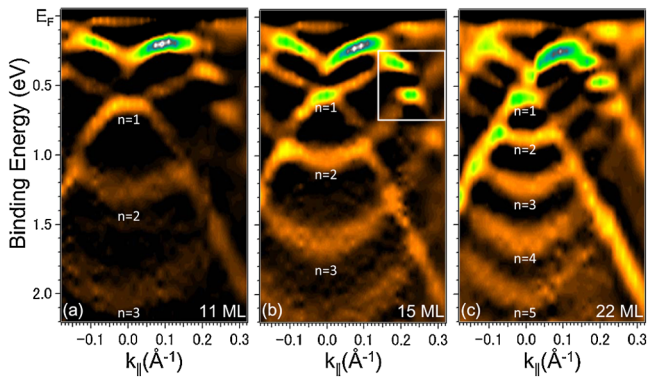

FIG. 2 (color online). $E_B - k_{\|}$ diagrams of $(\sqrt{3}\times\sqrt{3})$ $R30°$ Bi/Ag on Ag(111) films of (a) 11, (b) 15, and (c) 22 ML.

Modifications of band dispersions due to the interactions between SSs, QWSs, and substrate bands have been observed in several metal quantum well films. Unlike these interactions between spin-degenerate bands, in the present case the interaction is between a spin-polarized band and a spin-degenerate band, which is physically very intriguing. We have used a simple model to simulate the result of this kind of interaction. The Hamiltonian is written as $H = H_{ss} + H_{qws} + V$, where H_{ss} and H_{qws} are unperturbed energies of the spin-split SS and a QWS, respectively, and V is the interaction between them. It is actually an Anderson model [20] except that the correlation term is dropped. Since in this system both the SS and QWS are sp-like extended states, the effective Coulomb repulsion is negligible. The Hamiltonian can be written in a 4×4 matrix with four basis states $|SS\uparrow\rangle$, $|SS\downarrow\rangle$, $|QWS\uparrow\rangle$, and $|QWS\downarrow\rangle$, which are spin-up and spin-down states of SSs and QWSs. Diagonal components of the 4×4 matrix correspond to in-plane band energies of original SSs and QWSs. For the SS band, it is $E_{ss}^{\uparrow\downarrow}(k) = E_{ss0} + \hbar^2(k \pm k_0)^2/2m_{ss}^*$, and, for the QWS subbands, it is $E_{qws}^{\uparrow}(k) = E_{qws}^{\downarrow}(k) = E_{qws0} + \hbar^2k^2/2m_{qws}^*$. The effective masses of the SS (m_{ss}^*) and the QWS (m_{qws}^*) are determined from energy dispersion curves of the $(\sqrt{3}\times\sqrt{3})$ $R30°$ Bi/Ag surface formed on the bulk Ag(111) crystal and clean Ag(111) quantum film on Si(111)7×7, respectively. In the present simulation, we adopted $m_{ss}^* = 0.25\ m_e$ and $m_{qws}^* = 0.5\ m_e$, where m_e is the electron rest mass. In the energy of the original SS band, k_0 represents the size of the Rashba spin splitting, which is $k_0 = 0.13$ Å^{-1} [19]. E_{qws0} (E_{ss0}) is the binding energy of the QWS (SS) at $k = 0$ ($k = \pm k_0$).

The interaction between the SS and the QWS is expressed in off-diagonal terms: $\langle QWS\uparrow(\downarrow)|V|SS\uparrow(\downarrow)\rangle$ and $\langle QWS\uparrow(\downarrow)|V|SS\downarrow(\uparrow)\rangle$. The former and latter terms represent the interactions between states with the same spin and different spin, respectively. As discussed above, in this system, there are no d electrons involved, so the exchange and correlation energy are too small to induce a spin-flip process. Spin-orbit coupling is a single-body effect and therefore does not contribute to the interaction between the SS and the QWS. So the interaction between the SS and the QWS can be attributed only to hybridization. Hybridization takes place only between bands with the same spin [20,21]. So the $\langle QWS\uparrow(\downarrow)|V|SS\downarrow(\uparrow)\rangle$ terms should be near zero. Because of Kramer's degeneracy,

$\langle$QWS $\uparrow$ $|V|$SS $\uparrow\rangle$ equals $\langle$QWS $\downarrow$ $|V|$SS $\downarrow\rangle$ and is set as V_h. The band dispersion is obtained by diagonalizing the matrix with V_h as a fitting parameter.

The simulation results are presented in Figs. 3(a)–3(d). The solid lines depict the calculated band dispersions. The colors of the lines in Figs. 3(a)–3(d) indicate the weights of square amplitude of four basis components, respectively. Just as the experimental spectra, beyond the crossings between the SS and QWS bands, the band dispersions are nearly the same with the noninteracted SS and QWS. Around every crossing point, the SS is broken with a gap of $2 \mid V_h \mid$ [see Figs. 3(e) and 3(f)]. However, the QWS still remains in these gaps. Interestingly, in Figs. 3(c) and 3(d), one can see that in the gaps $|$QWS $\uparrow\rangle$ and $|$QWS $\downarrow\rangle$ show different weights. Namely, the QWS loses its spin degeneracy and processes a net spin in the gaps. We can find that the spin direction of the QWS in the gaps is just opposite to the spin of the SS band that it crosses. So the QWS is antiferromagnetically polarized by the spin-split SS due to the interaction. This result can be obtained only in the hybridization between a spin-degenerate band and a spin-polarized band. The simulation of the hybridization between two spin-degenerate bands shows that a real gap appears and there is no change in the spin polarization of the bands, which is similar with the usual anticrossing behavior [22,23]. The differences of the two cases are shown in Figs. 3(f) and 3(g). The spin polarization of the QWS originates from the fact that hybridization can take place only between states with the same spin. The spin-split SS interacts only with the QWS band with the same spin and forms gaps. At the same time, the QWS band with opposite spin remains unchanged in the hybridization gaps, resulting in the spin splitting. In some sense, this spin-polarization mechanism resembles the situation in $3d$ metals such as Ni, where the sp-d hybridization plays an important role in the induced exchange splitting of the sp bands [24,25].

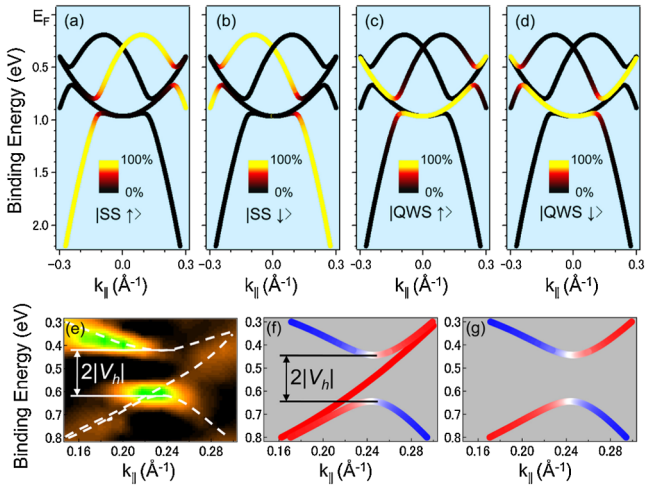

FIG. 3 (color online). (a)–(d) The simulated band maps with the weights (the color of the solid lines) of the four basis vectors: $|$SS $\uparrow\rangle$, $|$SS $\downarrow\rangle$, $|$QWS $\uparrow\rangle$, and $|$QWS $\downarrow\rangle$, respectively. (e) A close view of the measured band map in the region as indicated by the white box in Fig. 2(b). The white dashed lines are to guide the eyes. (f) The simulated band map at the same region with (e). (g) Same as (f) except assuming SS is spin-degenerated. The blue and red colors in (f) and (g) represent the weights of SS and QWS, respectively.

The splitting of QWSs is verified in the results of the first-principles calculations on $(\sqrt{3} \times \sqrt{3})$ $R30°$ Bi/Ag covered Ag(111) films [26,27]. From our ARPES data, the dispersions of QWS subbands seem not so obviously changed as that of the SS band, which is consistent with our simulation results. However, the fine structures around hybridization gaps can hardly be resolved due to the limitation of the measurement resolution. ARPES with higher resolution or/and spin resolution is expected to confirm the spin splittings of the QWSs.

In reality, neither the SS nor the QWSs are simply parabolic bands. The dispersions of QWS subbands are influenced by the bulk band edge of Si, leading to small kinks in QWS bands [14] as can be observed in Fig. 3(e). As for the spin-split SS bands, near the $\bar{\Gamma}$ point they are mainly sp_z states, while at large $k_\parallel$ they are mixture of sp_z states and $p_x p_y$ states [19,26]. The difference in the size of hybridization gaps between the outer and inner branches of the SS may come from the difference in the components of the two branches. These considerations will not essentially change the results of our simulation.

Figure 4(a) exhibits the dependence of $|V_h|$, i.e., half of the gap width, on the film thickness and quantum number of QWSs. The solid dots represent the experimental data determined from peak positions in ARPES spectra, as indicated by the pairs of dashed blue lines in Fig. 1(b). In Fig. 4(a), we show only the data of the interaction between the outer branches of the SS band and QWS bands. We can see that the gap width increases with increasing quantum number and decreasing film thickness. According to the present hybridization model, the gap width is $2|V_h| = 2|\langle$QWS $\uparrow$ $(\downarrow)|V|$SS $\uparrow$ $(\downarrow)\rangle|$. If V is simply set as a constant, the gap width will be proportional to the overlapping integral between SS and QWS wave functions: $2|V_h| = 2|V||\langle$QWS $\uparrow$ $(\downarrow)|$SS $\uparrow$ $(\downarrow)\rangle|$. For the integration, we insert a one-dimensional exponential function for the $|$SS$\rangle$ wave function and a one-dimensional sinusoidal function for the $|$QWS$\rangle$ wave function. The Bloch functions and the in-plane wave functions of SSs and QWSs are not considered since they change little with the parameters such as film thickness and quantum well number. The exact form of the sinusoidal function for a QWS is defined by film thickness, quantum number, and the phase shifts at the film-substrate and the film-vacuum interfaces. The film-substrate phase shift is set as -0.5π according to Ref. [28]. An example of the real-space features of the SS and QWS wave functions is depicted in Fig. 4(b). Figure 4(c) displays the calculated integrals for a 15 ML film with different quantum well

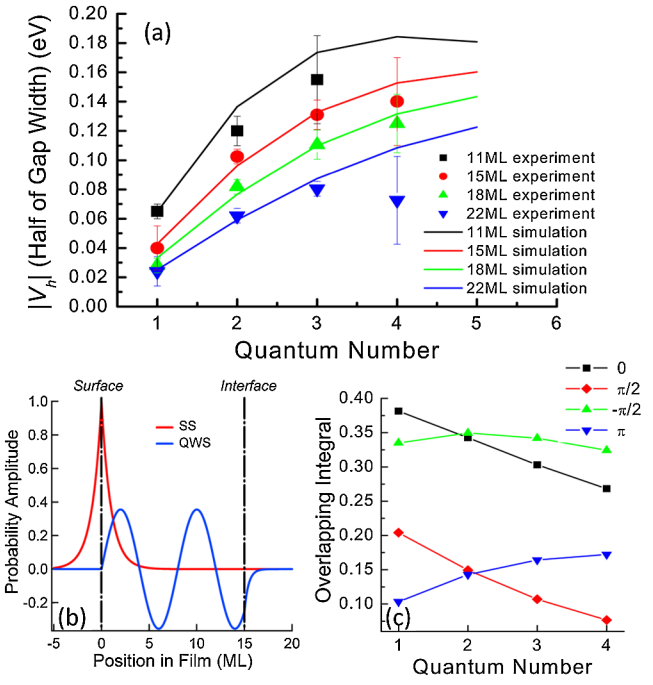

FIG. 4 (color online). (a) Evolution of the $|V_h|$ of $(\sqrt{3} \times \sqrt{3})$ $R30°$ Bi/Ag covered Ag(111) films with film thickness and quantum well number. (b) The real-space wave functions of the SS (solid red line) and QWS (solid blue line). The film thickness is 15 ML. The quantum well number is 4. The phase shifts at film-vacuum and film-substrate interfaces are π and -0.5π, respectively. (c) Calculated overlapping integrals of a $(\sqrt{3} \times \sqrt{3})$ $R30°$ Bi/Ag covered 15 ML Ag(111) film on different quantum well numbers and film-vacuum phase shifts.

numbers and film-vacuum phase shifts. The calculation results demonstrate that, for a film-vacuum phase shift around π, the overlapping integral has similar dependence on film thickness and quantum number as the experimental gap width data. The solid lines in Fig. 4(a) exhibit the $|V_h|$ obtained by multiplying the calculated overlapping integrals of different film thicknesses and quantum well numbers with the fitting parameter $V = 0.92$ eV. The results show fairly good agreement with the experimental data. So the gap width evolution can be understood as the result of the overlapping between QWS and SS wave functions and is consistent with the band hybridization model.

In summary, we studied the band structure of a $(\sqrt{3} \times \sqrt{3})$ $R30°$ Bi/Ag surface ordered alloy grown on Ag(111) quantum well films with ARPES. Gaps open in the spin-split SS where they cross the QWSs. The result is well reproduced with the band hybridization model, which implies that the QWSs be antiferromagnetically spin polarized by the spin-split SS in the hybridization gaps. The present research proposes a new mechanism to produce spin polarization in an nonmagnetic metal film on a semiconductor substrate.

We gratefully acknowledge G. Bihlmayer and E. V. Chulkov for their helpful discussions. This work has been supported by the Japanese Society for the Promotion of Science and JSPS-NSFC-KOSEF A3 Foresight Program.

[1] I. Zutic *et al.*, Rev. Mod. Phys. **76**, 323 (2004).
[2] Y. A. Bychkov and E. I. Rashba, JETP Lett. **39**, 78 (1984).
[3] M. I. Dyakonov and V. I. Perel, Fiz. Tverd. Tela (Leningrad) **13**, 3581 (1971).
[4] S. Datta and B. Das, Appl. Phys. Lett. **56**, 665 (1990).
[5] M. I. Dyakonov and V. I. Perel, Phys. Lett. **35**, 459 (1971).
[6] J. E. Hirsch, Phys. Rev. Lett. **83**, 1834 (1999).
[7] S. Zhang, Phys. Rev. Lett. **85**, 393 (2000).
[8] S. LaShell, B. A. McDougall, and E. Jensen, Phys. Rev. Lett. **77**, 3419 (1996).
[9] Y. M. Koroteev *et al.*, Phys. Rev. Lett. **93**, 046403 (2004).
[10] K. Sugawara *et al.*, Phys. Rev. Lett. **96**, 046411 (2006).
[11] J. Luo *et al.*, Phys. Rev. B **41**, 7685 (1990); **38**, 10 142 (1988).
[12] T. Hirahara *et al.*, Appl. Phys. Lett. **91**, 202106 (2007).
[13] I. Matsuda, T. Ohta, and H. W. Yeom, Phys. Rev. B **65**, 085327 (2002); I. Matsuda *et al.*, *ibid.* **63**, 125325 (2001).
[14] N. J. Speer *et al.*, Science **314**, 804 (2006); S.-J. Tang *et al.*, Phys. Rev. Lett. **96**, 216803 (2006); **96**, 036802 (2006); **93**, 216804 (2004).
[15] T. Hirahara *et al.*, Phys. Rev. Lett. **97**, 146803 (2006).
[16] L. Aballe *et al.*, Phys. Rev. Lett. **87**, 156801 (2001).
[17] F. Schiller *et al.*, Phys. Rev. Lett. **95**, 126402 (2005); C. Koitzsch *et al.*, Phys. Rev. Lett. **95**, 126401 (2005).
[18] T.-C. Chiang, Surf. Sci. Rep. **39**, 181 (2000).
[19] C. R. Ast *et al.*, Phys. Rev. Lett. **98**, 186807 (2007); arXiv: cond-mat/0509509.
[20] P. W. Anderson, Phys. Rev. **124**, 41 (1961).
[21] I. Barke *et al.*, Phys. Rev. Lett. **97**, 226405 (2006).
[22] C. Liu *et al.*, Phys. Rev. Lett. **96**, 036803 (2006).
[23] W. Shan *et al.*, Phys. Rev. Lett. **82**, 1221 (1999).
[24] L. Hodges *et al.*, Phys. Rev. **152**, 505 (1966).
[25] T. J. Kreutz *et al.*, Phys. Rev. B **58**, 1300 (1998).
[26] G. Bihlmayer, S. Blügel, and E. V. Chulkov, Phys. Rev. B **75**, 195414 (2007).
[27] It is of note that, in Ref. [26], the splitting of QWSs can be observed in Fig. 4 but not in Fig. 1. For Fig. 1, a symmetric film, with $(\sqrt{3} \times \sqrt{3})$ $R30°$ Bi/Ag on both of the surfaces, is used for calculation. In this case, the SSs from both surfaces are included in the results, and they are actually spin-degenerate in momentum space. Therefore the calculation result reveals the hybridization between two spin-degenerate bands.
[28] N. Nagamura *et al.*, Phys. Rev. Lett. **96**, 256801 (2006).